Distributed Adaptive Time-Varying Group Formation Tracking for Multiagent Systems With Multiple Leaders on Directed Graphs

Junyan Hu, Parijat Bhowmick, and Alexander Lanzon, *Senior Member, IEEE*

***Abstract*—This paper proposes a fully distributed control protocol that achieves time-varying group formation tracking for linear multiagent systems connected via a directed graph. The group formation tracking often leads to sub-formations especially when the leaders are placed far apart or they have separate control inputs. In the proposed approach, the followers are distributed into several subgroups and each subgroup attains the predefined subformation along with encompassing the leaders. Each subgroup can be assigned multiple leaders, contrary to the single-leader case considered in most existing literature, which makes the current problem nontrivial. When multiple leaders exist in a subgroup, the subformation attained by that subgroup keeps tracking a convex combination of the states of the leaders. A distributed adaptive control protocol has been introduced in this paper which uses only relative state information and, thus, avoids direct computation of the graph Laplacian matrix. Due to the virtue of this, the proposed scheme remains effective even when some of the agents get disconnected from the network due to sudden communication failure. An algorithm is provided to outline the steps to design the control law to attain time-varying group formation tracking with multiple leaders. Toward the end, a case study on multitarget surveillance operation is taken up to show an important application of the proposed adaptive control technique.**

***Index Terms*—Adaptive consensus, cooperative control, group formation, multiagent systems (MAS), swarm robotics.**

I. Introduction

OVER THE past two decades, cooperative as well as distributed control of multiagent systems (MAS) have drawn significant attention of researchers from multiple disciplines of engineering and mathematics because of its wide applications in multirobot cooperation [1]–[3]; distributed sensor networks [4], [5]; renewable energy storage systems [6]; etc. This research domain primarily includes three topics: 1) consensus control [7]–[9]; 2) containment control [10]; and 3) formation control [11]. Among them, formation control of MAS is a potential field of research that has witnessed an immense growth in the last 15 years [12]. Time-invariant formation control of a swarm of quad-rotors has been reported in [13], while formation control of MAS on a time-varying trajectory is still an important issue which requires further attention.

Time-varying formation control of MAS involves a rate of change of the formation states, which causes major challenges to design distributed control schemes. A "bearing-based formation control" of a swarm of single integrator agents was introduced in [14] using the leader-first follower structure. Fixed-time formation control of an assembly of moving robots considering the time-delay constraint was analyzed in [15]. Dynamic formation control for second-order MAS using the graph Laplacian approach was studied in [16]. In [17], an affine formation maneuver control technique was proposed to configure a particular geometric pattern by the agents while achieving the desired maneuvers. Subsequently, time-varying formation control with an application to unmanned aerial vehicles is investigated in [18]–[20]. However, in [18]–[20], the proposed control protocols utilize the smallest nonzero eigenvalue of the graph Laplacian matrix which indicates that the control schemes are not fully distributed [21]. To circumvent direct computation of the eigenvalues of the graph Laplacian matrix, distributed control protocols are now being widely used which depend only on the local information, that is, information from the neighbors. In this context, the work of [22] should be highlighted which proposes a fully distributed control protocol for MAS with an undirected graph. However, it has been found that MAS on undirected graphs suffer from a lack of robustness and reliability especially when communication failure occurs and some of the agents get disconnected, resulting in a change in the graph topology [21]. On the contrary, MAS connected via directed graphs are more reliable and offer some robustness to topology changes. In [23], a fully distributed control scheme was introduced to solve the output regulation problem for linear and heterogeneous MAS on a directed communication graph.

Formation control of MAS with a single leader has been studied extensively in [14]–[20], while a formation tracking problem with multiple leaders is a relatively unexplored area which needs

Manuscript received November 9, 2018; revised November 13, 2018 and February 18, 2019; accepted April 7, 2019. Date of publication April 26, 2019; date of current version March 18, 2020. This work was supported by the Engineering and Physical Sciences Research Council (EPSRC) [Grant EP/R008876/1]. Recommended by Associate Editor Y. Paschalidis. *(Corresponding author: Junyan Hu.)*

The authors are with the Control Systems Centre, School of Electrical and Electronic Engineering, University of Manchester, Manchester M13 9PL, U.K. (e-mail: Junyan.hu@manchester.ac.uk; Parijat.bhowmick@manchester.ac.uk; Alexander.lanzon@manchester.ac.uk).

Digital Object Identifier 10.1109/TCNS.2019.2913619

more effort. Formation and tracking control of MAS having multiple targets (considered as leaders) are nontrivial and relatively more complex than single-leader operations [21]. Very often, in order to accomplish distributed tasks, a MAS may need to be decomposed into several subgroups, where each subgroup may contain multiple leaders. In the literature, the topic "group formation tracking" deals with formation tracking of MAS containing multiple subgroups. In contrast to "complete formation" which deals with only a single group, "group formation" is more complicated and challenging since the latter involves interactions within each subgroup as well as among the subgroups and multiple "subformations". However, in many recent papers, for instance in [14]–[20], only formation tracking control problems are considered which urges more attention toward solving the group formation tracking problems. Applications like search-and-rescue operations, multitarget surveillances, etc., extensively rely on group formation tracking concepts involving multiple leaders where the leaders may also have some exogenous inputs. In [24]–[27], group consensus control problems specialized to first-order and second-order MAS have been addressed, but the techniques in general cannot be applied directly to solve time-varying group formation tracking (TGFT) problems for higher-order MAS. Thus, the problem of distributed TGFT, where each subgroup may have multiple leaders (or targets), deserves further research.

The aforementioned issues motivate us to investigate the TGFT problems for linear MAS on a directed graph containing multiple leaders. The primary objective is to spread the agents into several subgroups and to achieve subformation for each individual subgroup along with reference tracking. It is shown that consensus control, formation control, and cluster control can all be viewed as particular scenarios of the TGFT problem addressed in this paper. The contributions of this paper can be summarized as follows:

1) The TGFT problem for MAS with a directed communication graph is explored, where each subgroup is able to reach a desired subformation surrounding the respective leaders. In contrast with the existing literature, in this paper, each subgroup can be assigned multiple leaders and the leaders may be subjected to bounded exogenous (either reference or disturbance) inputs independent of the other agents and their interactions.
2) The TGFT control protocol proposed in this paper does not require the information about the entire graph, unlike most of the existing formation control strategies. The proposed control law uses only the relative state information and thereby avoids explicit computation of the eigenvalues of the graph Laplacian matrix. As a result, the control architecture becomes fully distributed, reconfigurable, and scalable for large-scale networked systems.

The rest of the paper proceeds as follows. Section II covers the preliminaries and background and discusses the problem statement. In Section III, the TGFT problem is solved via a Lyapunov approach using a nonlinear, adaptive, and distributed control law. A case study on a multitarget surveillance problem is given in Section IV to highlight a potential application of the proposed scheme. Section V concludes this paper, mentioning several future research directions.

The notations and acronyms are standard throughout. $\mathbb{R}$ denotes the set of all real numbers. $\mathbb{R}_{>0}$ and $\mathbb{R}_{\geq 0}$ denote, respectively, the sets of all positive and all non-negative real numbers. Let $I_{n\times n}$ denote the identity matrix and $\mathbf{1}_N$ be a shorthand for $[1,\ldots,1]^T_{1\times N}$. $\text{diag}\{a_i\}$ represents a diagonal matrix with diagonal entries a_i. The Kronecker product of two matrices A and B is denoted by $A\otimes B$. $\|.\|$ expresses the 2-norm of a vector or a matrix. A square matrix $A\in\mathbb{R}^{n\times n}$ is called a nonsingular M-matrix if all of its off-diagonal elements are nonpositive and all eigenvalues of A have positive real parts [21].

II. Preliminaries and Problem Formulation

A. Graph Theory

Let $\mathcal{G}=(\mathcal{V},\mathcal{E},\mathcal{A})$ be a weighted and directed graph for which $\mathcal{V}=\{1,2,\ldots,N\}$ is a nonempty set of nodes, $\mathcal{E}\subset\mathcal{V}\times\mathcal{V}$ is the set of edges and $\mathcal{A}=[a_{ij}]\in\mathbb{R}^{N\times N}$ is the adjacency matrix corresponding to the graph. An edge denoted by (i,j) indicates that information flows from node i to node j and, in this case, node i is considered as a neighbor of node j. a_{ij} is the weight of edge (j,i) and $a_{ij}\neq 0$ if $(j,i)\in\mathcal{E}$. The in-degree matrix associated with $\mathcal{G}$ is defined as $D=\text{diag}\{d_i\}\in\mathbb{R}^{N\times N}$ with $d_i=\sum_{j=1}^{N}a_{ij}$ and the Laplacian matrix $L\in\mathbb{R}^{N\times N}$ of $\mathcal{G}$ is given by $L=D-\mathcal{A}$. Within a directed graph, a spanning tree exists if the graph has a "root" node having a directed path to each of the remaining nodes. A directed graph without any cycle is called the "directed acyclic graph".

Consider that a MAS is comprised of N agents, including M followers and $N-M$ leaders. Let $F=\{1,2,\ldots,M\}$ and $E=\{M+1,M+2,\ldots,N\}$ be the sets of the followers and leaders, respectively. For any $i,j\in\{1,2,\ldots,N\}$, the weight of an interaction edge w_{ij} is defined as

$$w_{ij}=\begin{cases}0 \text{ when } i=j \text{ or } (j,i)\notin\mathcal{E},\\ b_j \text{ when } j\in E \text{ and } (j,i)\in\mathcal{E},\\ a_{ij} \text{ when both } i,j\in F \text{ and } (j,i)\in\mathcal{E}\end{cases} \quad (1)$$

where $b_j\in\mathbb{R}_{>0}$ and $a_{ij}\in\mathbb{R}$ are known constants for all i and j.

Lemma 1: [28] Let $L\in\mathbb{R}^{n\times n}$ be an M-matrix with $\det[L]\neq 0$. Then, there exists a positive-definite matrix $G=\text{diag}\{g_1,\ldots,g_N\}$ such that $GL+L^TG>0$.

Lemma 2: [29] Suppose $a\in\mathbb{R}_{\geq 0}$, $b\in\mathbb{R}_{\geq 0}$, $p\in\mathbb{R}_{>0}$ and $q\in\mathbb{R}_{>0}$ such that $\frac{1}{p}+\frac{1}{q}=1$, then $ab\leq\frac{a^p}{p}+\frac{b^q}{q}$. Moreover, $ab=\frac{a^p}{p}+\frac{b^q}{q}$ if and only if $a^p=b^q$.

B. Problem Formulation

The homogeneous leader and follower agents are described by the state-space equations

$$\dot{x}_i(t)=Ax_i(t)+Bu_i(t)\ \forall i\in\{1,2,\ldots,N\} \quad (2)$$

where $x_i(t) \in \mathbb{R}^n$ and $u_i(t) \in \mathbb{R}^m$ are, respectively, the state and control input vectors of the ith agent $\forall t \geq 0$. $A \in \mathbb{R}^{n\times n}$ and $B \in \mathbb{R}^{n\times m}$ are constant matrices where $\operatorname{rank}(B) = m$, $m \leq n$ and (A, B) are stabilizable.

Assumption 1: Let $u_k(t)\ \forall k \in E$ represent the exogenous input for the kth leader which is independent of all other agents and the network topology. We assume $\|u_k(t)\| \leq \sigma$ for all $t \geq 0$ for a given $\sigma \in \mathbb{R}_{\geq 0}$.

Then, the Laplacian matrix L corresponding to the graph $\mathcal{G}$ can be partitioned as $[L = \begin{smallmatrix} L_1 & L_2 \\ 0_{(N-M)\times M} & 0_{(N-M)\times(N-M)} \end{smallmatrix}]$, where $L_1 \in \mathbb{R}^{M\times M}$ and $L_2 \in \mathbb{R}^{M\times(N-M)}$.

Let $h_F(t) = \left[h_1^T(t), h_2^T(t), \ldots, h_M^T(t)\right]^T$ generate the desired formation where $h_i(t) \in \mathbb{R}^n$ for all $t \geq 0$ and all $i \in \{1, \ldots, M\}$ is a preset vector known to the ith follower.

The problem statement considered here is to develop a fully distributed control technique for an MAS given in (2) to achieve subformations when the followers are divided into several subgroups and each subgroup is assigned one or multiple leaders to track. Motivated by [30], a TGFT control protocol is constructed below

$$\begin{cases} u_i = (c_i + \rho_i)K\xi_i + \gamma_i - \mu f(\xi_i) \\ \dot{c}_i = \xi_i^T \Gamma \xi_i \end{cases} \quad \forall i \in F \tag{3}$$

where $\xi_i = \sum_{j=1}^{M} w_{ij}[(x_i - h_i) - (x_j - h_j)] + \sum_{k=M+1}^{N} w_{ik}[(x_i - h_i) - x_k]$ denotes the group formation tracking error; $c_i(t)$ with $c_i(0) > 0$ represents the coupling weight assigned to the ith agent; $\mu > 0$, $K \in \mathbb{R}^{m\times n}$ and $\Gamma \in \mathbb{R}^{n\times n}$ are all constant controller parameters to be selected appropriately; ρ_i and γ_i are continuously differentiable functions of ξ_i and h_i respectively; and $f(\cdot)$ is a nonlinear function to be determined later.

Let $x_F = \left[x_1^T, \ldots, x_M^T\right]^T$, $x_E = \left[x_{M+1}^T, \ldots, x_N^T\right]^T$, $u_E = \left[u_{M+1}^T, \ldots, u_N^T\right]^T$, $\gamma = \left[\gamma_1^T, \gamma_2^T, \ldots, \gamma_M^T\right]^T$ and $F(\xi) = \left[f^T(\xi_1), f^T(\xi_2), \ldots, f^T(\xi_M)\right]^T$ denote a few shorthand. The closed-loop system dynamics of the MAS (2) embedded with the TGFT control protocol (3) can be expressed in a structured form as

$$\begin{cases} \dot{x}_F = \left[I_M \otimes A + (C+\rho)L_1 \otimes BK\right]x_F \\ \qquad + \left[(C+\rho)L_2 \otimes BK\right]x_E + (I_M \otimes B)\gamma \\ \qquad - \left[(C+\rho)L_1 \otimes BK\right]h_F - \mu(I_M \otimes B)F(\xi), \\ \dot{x}_E = (I_{N-M} \otimes A)x_E + (I_{N-M} \otimes B)u_E \end{cases} \tag{4}$$

where $C = \operatorname{diag}\{c_1, \ldots, c_M\}$ and $\rho = \operatorname{diag}\{\rho_1, \ldots, \rho_M\}$.

III. Main Results

Suppose the MAS (2) is decomposed into p subgroups $(p \geq 1)$ and accordingly, the node set $\mathcal{V}$ consists of $\mathcal{V}_1, \ldots, \mathcal{V}_p$ satisfying $\mathcal{V}_k \neq \emptyset$, $\mathcal{V} = \bigcup_{k=1}^{p} \mathcal{V}_k$ and $\mathcal{V}_k \bigcap \mathcal{V}_l = \emptyset$ for any $k, l \in \{1, 2, \ldots, p\}$ and $k \neq l$. Let $\bar{i} \in \{1, 2, \ldots, p\}$ denote the subscript of a subgroup and $\mathcal{G}_{\bar{i}}$ represents the part of the entire graph $\mathcal{G}$ which corresponds to the subgroup $V_{\bar{i}}$. $n_{\bar{i}}$ and $\hat{n}_{\bar{i}}$ denote, respectively, the numbers of followers and leaders in the subgroup $\mathcal{V}_{\bar{i}}$. Note, in an MAS, a leader agent must not have any neighbor, while a follower agent should have at least one neighbor. A follower is said to be "well-informed" if it is connected to all leaders and "uninformed" if it is not connected to any of the leaders.

Assumption 2: For each subgroup, at least one leader should exist which provides a reference trajectory to the followers. Any follower in a given subgroup is assumed to be either well-informed or uninformed. If a follower belongs to the uninformed category, then it is connected to at least one well-informed follower via a directed path to it.

Assumption 3: The subsets $\mathcal{V}_1, \mathcal{V}_2, \ldots, \mathcal{V}_p$ of the node set $\mathcal{V}$ do not form any cycle among them.

Based on Assumption 3, L_1 has a particular structure as shown below [26]

$$L_1 = \begin{bmatrix} L_{11} & 0 & \cdots & 0 \\ L_{21} & L_{22} & \cdots & 0 \\ \vdots & \vdots & \ddots & \vdots \\ L_{p1} & L_{p2} & \cdots & L_{pp} \end{bmatrix} \tag{5}$$

where $L_{\bar{i}\bar{i}}$ is the Laplacian matrix corresponding to $\mathcal{G}_{\bar{i}}$, and $L_{\bar{i}\bar{j}}$ and $L_{\bar{j}\bar{i}}$ together express the mutual interaction between the $\bar{i}$th and $\bar{j}$th subgroups, where $\bar{i}, \bar{j} \in \{1, \ldots, p\}$, and $\bar{i} \neq \bar{j}$.

Assumption 4: Every row-sum of $L_{\bar{i}\bar{j}}$ is zero when $\bar{j} < \bar{i}$ for $\bar{i}, \bar{j} \in \{1, \ldots, p\}$.

Remark 1: If two subgroups are connected via positive edges (i.e., edges having positive weights), then the subgroups interact in a "cooperative" relation. On the contrary, if they are connected via negative edges, then the subgroups respond to each other in a "competitive" relation. Both of these modes exist together in an MAS and ensure that all subgroups work in unison to achieve individual subformations along with tracking the respective leaders.

For any subgroup $\bar{i} \in \{1, 2, \ldots, p\}$, the desired time-varying subformation is characterized by the vector $\bar{h}_{\bar{i}}(t) = \left[h_{\varsigma_{\bar{i}}+1}^T(t), h_{\varsigma_{\bar{i}}+2}^T(t), \ldots, h_{\varsigma_{\bar{i}}+n_{\bar{i}}}^T(t)\right]^T$, where $\varsigma_{\bar{i}} = \sum_{k=0}^{\bar{i}-1} n_k$ with $n_0 = 0$ and each element in $\bar{h}_{\bar{i}}(t)$ is piece-wise continuously differentiable. It can be readily verified that $h_F(t) = \left[\bar{h}_1^T(t), \bar{h}_2^T(t), \ldots, \bar{h}_p^T(t)\right]^T$ reflects the formation vector for the entire MAS (2). $\bar{x}_{\bar{i}} = \left[x_{\varsigma_{\bar{i}}+1}^T(t), x_{\varsigma_{\bar{i}}+2}^T(t), \ldots, x_{\varsigma_{\bar{i}}+n_{\bar{i}}}^T(t)\right]^T$ and $\hat{x}_{\bar{i}} = \left[x_{\hat{\varsigma}_{\bar{i}}+1}^T(t), x_{\hat{\varsigma}_{\bar{i}}+2}^T(t), \ldots, x_{\hat{\varsigma}_{\bar{i}}+\hat{n}_{\bar{i}}}^T(t)\right]^T$ represent the state vector of the followers and the leaders, respectively, of the $\bar{i}$th subgroup, where $\hat{\varsigma}_{\bar{i}} = M + \sum_{k=0}^{\bar{i}-1} \hat{n}_k$ with $\hat{n}_0 = 0$.

Lemma 3: If Assumptions 2-4 are satisfied, then $-L_1^{-1}L_2$ has the following form:

$$-L_1^{-1}L_2 = \begin{bmatrix} e_1 & 0 & \cdots & 0 \\ 0 & e_2 & \cdots & 0 \\ \vdots & \vdots & \ddots & \vdots \\ 0 & 0 & \cdots & e_p \end{bmatrix} \tag{6}$$

where $e_{\bar{i}} = \mathbf{1}_{n_{\bar{i}}}[b_{\hat{\varsigma}_{\bar{i}}+1}, b_{\hat{\varsigma}_{\bar{i}}+2}, \ldots, b_{\hat{\varsigma}_{\bar{i}}+\hat{n}_{\bar{i}}}]/\sum_{k=\hat{\varsigma}_{\bar{i}}+1}^{\hat{\varsigma}_{\bar{i}}+\hat{n}_{\bar{i}}} b_k$.

Proof: We start with only one leader associated with each subgroup. For the $\bar{i}$th subgroup, let the vector $\hat{e}_{\bar{i}} \in \mathbb{R}^{n_{\bar{i}}}$ have $w_{(\varsigma_{\bar{i}}+i)(M+\bar{i})}$ as its ith element if the ith agent of this subgroup observes the leader, and all other entries are 0. If Assumptions 2–4 hold, then $L_{\bar{i}\bar{i}}$ is nonsingular $\forall \bar{i} \in \{1,\ldots,p\}$ and we can express $\hat{e}_{\bar{i}} = L_{\bar{i}\bar{i}}\mathbf{1}_{n_{\bar{i}}}$, which readily implies

$$L_{\bar{i}\bar{i}}^{-1}\hat{e}_{\bar{i}} = \mathbf{1}_{n_{\bar{i}}}. \tag{7}$$

Postmultiplying both sides of (7) by $b_j/\sum_{k=\hat{\varsigma}_{\bar{i}}+1}^{\hat{\varsigma}_{\bar{i}}+\hat{n}_{\bar{i}}} b_k$, we get

$$L_{\bar{i}\bar{i}}^{-1}\hat{e}_{\bar{i}}\left(b_j\Big/\sum_{k=\hat{\varsigma}_{\bar{i}}+1}^{\hat{\varsigma}_{\bar{i}}+\hat{n}_{\bar{i}}} b_k\right) = \mathbf{1}_{n_{\bar{i}}}\left(b_j\sum_{k=\hat{\varsigma}_{\bar{i}}+1}^{\hat{\varsigma}_{\bar{i}}+\hat{n}_{\bar{i}}} b_k\right). \tag{8}$$

It can be found that

$$\begin{aligned}&\sum_{j=\hat{\varsigma}_{\bar{i}}+1}^{\hat{\varsigma}_{\bar{i}}+\hat{n}_{\bar{i}}}\left(\mathbf{1}_{n_{\bar{i}}}(b_j\Big/\sum_{k=\hat{\varsigma}_{\bar{i}}+1}^{\hat{\varsigma}_{\bar{i}}+\hat{n}_{\bar{i}}} b_k)\right)\\ &= \left(1\Big/\sum_{k=\hat{\varsigma}_{\bar{i}}+1}^{\hat{\varsigma}_{\bar{i}}+\hat{n}_{\bar{i}}} b_k\right)(\mathbf{1}_{n_{\bar{i}}}\otimes[b_{\hat{\varsigma}_{\bar{i}}+1}, b_{\hat{\varsigma}_{\bar{i}}+2},\ldots,b_{\hat{\varsigma}_{\bar{i}}+\hat{n}_{\bar{i}}}])\\ &= e_{\bar{i}}.\end{aligned} \tag{9}$$

From (8) and (9), we have

$$L_{\bar{i}\bar{i}}e_{\bar{i}} = \sum_{j=\hat{\varsigma}_{\bar{i}}+1}^{\hat{\varsigma}_{\bar{i}}+\hat{n}_{\bar{i}}}\hat{e}_{\bar{i}}\left(b_j\Big/\sum_{k=\hat{\varsigma}_{\bar{i}}+1}^{\hat{\varsigma}_{\bar{i}}+\hat{n}_{\bar{i}}} b_k\right). \tag{10}$$

Then, we have

$$\begin{aligned}&L_1\begin{bmatrix} e_1 & 0 & \cdots & 0\\ 0 & e_2 & \cdots & 0\\ \vdots & \vdots & \ddots & \vdots\\ 0 & 0 & \cdots & e_p\end{bmatrix}\\ &= \begin{bmatrix} L_{11}e_1 & 0 & \cdots & 0\\ 0 & L_{22}e_2 & \cdots & 0\\ \vdots & \vdots & \ddots & \vdots\\ 0 & 0 & \cdots & L_{pp}e_p\end{bmatrix}\\ &= -L_2.\end{aligned} \tag{11}$$

Since L_1 is nonsingular, the conclusion is straightforward from (11). ■

An MAS is said to achieve TGFT with multiple leaders if for any given bounded initial states

$$\lim_{t\to\infty}\left(\bar{x}_{\bar{i}}(t) - \bar{h}_{\bar{i}}(t) - \mathbf{1}_{n_{\bar{i}}}\sum_{k=\hat{\varsigma}_{\bar{i}}+1}^{\hat{\varsigma}_{\bar{i}}+\hat{n}_{\bar{i}}}\alpha_k x_k(t)\right) = 0 \tag{12}$$

for all $\bar{i} \in \{1,2,\ldots,p\}$, where α_k is a positive constant that satisfies $\sum_{k=\hat{\varsigma}_{\bar{i}}+1}^{\hat{\varsigma}_{\bar{i}}+\hat{n}_{\bar{i}}}\alpha_k = 1$.

Since B is assumed to have full rank m, there exists the pseudoinverse $\tilde{B} \in \mathbb{R}^{m\times n}$ such that $\tilde{B}B = I_m$. We can also choose another matrix $\bar{B} \in \mathbb{R}^{(n-m)\times n}$, depending on the left null space of B such that $\bar{B}B = 0$ and $\left[\tilde{B}^T, \bar{B}^T\right]^T$ is nonsingular.

Theorem 1 is the main contribution of this paper which establishes the conditions to be satisfied by the MAS (2) to achieve TGFT by applying the fully distributed and nonlinear control protocol proposed in (3), provided the agents and the network hold certain properties. Moreover, the leaders are subjected to exogenous (either reference or disturbance) inputs independent of the dynamics of the agents and the network topology.

Theorem 1: Suppose Assumptions 1–4 hold and for a given $\sigma \geq 0$, the positive constant μ satisfies

$$\mu > \sigma. \tag{13}$$

If the following formation feasibility condition:

$$\bar{B}Ah_i - \bar{B}\dot{h}_i = 0 \tag{14}$$

is satisfied for a given set of $h_i(t) \in \mathbb{R}^n$ for all $t \geq 0$ and for all $i \in F$, then TGFT is achieved by the MAS (2) on applying the fully distributed and nonlinear control protocol given in (3) with $K = -R^{-1}B^TP$, $\Gamma = PBR^{-1}B^TP$, $\gamma_i = \tilde{B}\dot{h}_i - \tilde{B}Ah_i$ and $\rho_i = \xi_i^TP\xi_i$, where $P > 0$ is the solution of the algebraic Riccati (ARE) equation

$$A^TP + PA + Q - PBR^{-1}B^TP = 0 \tag{15}$$

for given $Q > 0$ and $R > 0$. The nonlinear function $f(\cdot)$ used in (3) is specified as

$$f(\xi_i(t)) = \begin{cases}\frac{B^TP\xi_i(t)}{\|B^TP\xi_i(t)\|} & \text{when } \left\|B^TP\xi_i(t)\right\| \neq 0;\\ 0 & \text{when } \left\|B^TP\xi_i(t)\right\| = 0;\end{cases} \tag{16}$$

for all $i \in F$.

Proof: Since via Assumption 2, each subgroup contains a directed spanning tree, it can be proved that all eigenvalues of $L_{\bar{i}\bar{i}}$ have a positive real part for all $\bar{i} \in \{1,\ldots,p\}$ [21]. By applying Lemma 1, there exists a real diagonal matrix $\Xi_{\bar{i}} > 0$ such that

$$\Xi_{\bar{i}}L_{\bar{i}\bar{i}} + L_{\bar{i}\bar{i}}^T\Xi_{\bar{i}} > 0\ \forall \bar{i} \in \{1,2,\ldots,p\}. \tag{17}$$

Define block diagonal matrices $\Xi = \operatorname{diag}\{\Xi_1,\ldots,\Xi_p\}$ and $\Delta = \operatorname{diag}\{\delta_1 I_{n_1},\ldots,\delta_p I_{n_p}\}$, where $\delta_{\bar{i}} > 0$ are required to be chosen such that $\Delta\Xi L_1 + L_1^T\Delta\Xi > 0$ holds. Now, we will show that there always exists a set of $\delta = \{\delta_1,\ldots,\delta_p\}$ such that the relation $\Delta\Xi L_1 + L_1^T\Delta\Xi > 0$ holds.

Let $\Theta_{\bar{i}} = \Xi_{\bar{i}}L_{\bar{i}\bar{i}} + L_{\bar{i}\bar{i}}^T\Xi_{\bar{i}}$ and

$$\Phi_{\bar{i}} = \begin{bmatrix}\delta_1\Theta_1 & \delta_2 L_{21}^T\Xi_2 & \cdots & \delta_{\bar{i}}L_{\bar{i}1}^T\Xi_{\bar{i}}\\ \delta_2\Xi_2L_{21} & \delta_2\Theta_2 & \cdots & \delta_{\bar{i}}L_{\bar{i}2}^T\Xi_{\bar{i}}\\ \vdots & \vdots & \ddots & \vdots\\ \delta_{\bar{i}}\Xi_{\bar{i}}L_{\bar{i}1} & \delta_{\bar{i}}\Xi_{\bar{i}}L_{\bar{i}2} & \cdots & \delta_{\bar{i}}\Theta_{\bar{i}}\end{bmatrix}\ \forall \bar{i} \in \{1,\ldots,p\}.$$

For $\bar{i}=2$, by applying the Schur Complement Lemma [31], we obtain $\Phi_2>0$ if and only if there exist $\delta_1>0$ and $\delta_2>0$ such that $\delta_1\Theta_1>0$ and

$$\delta_1\Theta_1-\delta_2 L_{21}^T\Xi_2\Theta_2^{-1}\Xi_2 L_{21}>0. \tag{18}$$

Since $\Theta_1>0$ and $\Theta_2>0$ via (17), we can always find a δ_2 sufficiently smaller than δ_1 such that (18) holds. The same arguments can be pursued to prove [26] that there always exist $\delta_1>\delta_2>\cdots>\delta_p$ such that $\Phi_p=\Delta\Xi L_1+L_1^T\Delta\Xi>0$, invoking (17).

Let the global formation tracking error be $\xi_F=[\xi_1^T,\ldots,\xi_M^T]^T$. Define $z_i=x_i-h_i\ \forall i\in F$ and $z_F=[z_1^T,\ldots,z_M^T]^T$. Now ξ_F can be written in a compact form as

$$\xi_F=(L_1\otimes I_n)z_F+(L_2\otimes I_n)x_E. \tag{19}$$

Substituting (4) into the derivative of (19), the expressions for $\dot{\xi}_F$ and $\dot{c}_i$ are obtained as

$$\begin{cases}\dot{\xi}_F=\left[I_M\otimes A+L_1(C+\rho)\otimes BK\right]\xi_F+(L_1\otimes A)h_F\\ \qquad -(L_1\otimes I_n)\dot{h}_F+(L_1\otimes B)\gamma+(L_2\otimes B)u_E\\ \qquad -\mu(L_1\otimes B)F(\xi),\\ \dot{c}_i=\xi_i^T\Gamma\xi_i.\end{cases} \tag{20}$$

Consider the following Lyapunov function candidate:

$$V_1=\sum_{i=1}^M\frac{1}{2}\varphi_i(2c_i+\rho_i)\rho_i+\frac{1}{2}\sum_{i=1}^M\varphi_i(c_i-\beta)^2 \tag{21}$$

where $\Delta\Xi=\mathrm{diag}\{\varphi_1,\ldots,\varphi_M\}$ is a positive-definite matrix with $\varphi_i\in\mathbb{R}_{>0}\ \forall i\in F$ such that $\Delta\Xi L_1+L_1^T\Delta\Xi>0$, and β is a positive constant to be determined later. As $c_i(0)>0$ for all $i\in F$, it follows from $\dot{c}_i(t)\geq 0$ that $c_i(t)>0$ for all $t>0$. Therefore, V_1 is positive definite and $V_1=0$ when $\xi_i=0$ $\forall i\in F$.

Now, the time derivative of V_1 along any trajectory of (20) is given by

$$\begin{aligned}\dot{V}_1&=\sum_{i=1}^M[\varphi_i(c_i+\rho_i)\dot{\rho}_i+\varphi_i\rho_i\dot{c}_i]+\sum_{i=1}^M\varphi_i(c_i-\beta)\dot{c}_i\\ &=\sum_{i=1}^M 2\varphi_i(c_i+\rho_i)\xi_i^TP\dot{\xi}_i+\sum_{i=1}^M\varphi_i(\rho_i+c_i-\beta)\dot{c}_i.\end{aligned} \tag{22}$$

Note that

$$\sum_{i=1}^M\varphi_i(\rho_i+c_i-\beta)\dot{c}_i={\xi_F}^T[(C+\rho-\beta I)\Delta\Xi\otimes\Gamma]\xi_F \tag{23}$$

and

$$\begin{aligned}\sum_{i=1}^M 2\varphi_i(c_i+\rho_i)\xi_i^TP\dot{\xi}_i&=2{\xi_F}^T[(C+\rho)\Delta\Xi\otimes P]\dot{\xi}_F\\ &={\xi_F}^T[(C+\rho)\Delta\Xi\otimes(PA+A^TP)\\ &\quad-(C+\rho)(\Delta\Xi L_1+L_1^T\Delta\Xi)(C+\rho)\otimes\Gamma]\xi_F\\ &\quad+2\xi_F^T[(C+\rho)\Delta\Xi L_1\otimes PA]h_F\\ &\quad-2\xi_F^T[(C+\rho)\Delta\Xi L_1\otimes P]\dot{h}_F\\ &\quad+2\xi_F^T[(C+\rho)\Delta\Xi L_1\otimes PB]\gamma\\ &\quad+2\xi_F^T[(C+\rho)\Delta\Xi L_2\otimes PB]u_E\\ &\quad-2\mu\xi_F^T[(C+\rho)\Delta\Xi L_1\otimes PB]F(\xi)\\ &\leq{\xi_F}^T[(C+\rho)\Delta\Xi\otimes(PA+A^TP)\\ &\quad-\lambda_1^{\min}(C+\rho)^2\otimes\Gamma]\xi_F\\ &\quad+2\xi_F^T[(C+\rho)\Delta\Xi L_1\otimes PA]h_F\\ &\quad-2\xi_F^T[(C+\rho)\Delta\Xi L_1\otimes P]\dot{h}_F\\ &\quad+2\xi_F^T[(C+\rho)\Delta\Xi L_1\otimes PB]\gamma\\ &\quad+2\xi_F^T[(C+\rho)\Delta\Xi L_2\otimes PB]u_E\\ &\quad-2\mu\xi_F^T[(C+\rho)\Delta\Xi L_1\otimes PB]F(\xi)\end{aligned} \tag{24}$$

where $\lambda_1^{\min}$ represents the smallest positive eigenvalue of $\Delta\Xi L_1+L_1^T\Delta\Xi$.

If condition (14) holds, then we have

$$\bar{B}Ah_i-\bar{B}\dot{h}_i+\bar{B}B\gamma_i=0 \tag{25}$$

since $\bar{B}B=0$. On letting $\gamma_i=\tilde{B}\dot{h}_i-\tilde{B}Ah_i\ \forall i\in F$, it follows that:

$$\tilde{B}Ah_i-\tilde{B}\dot{h}_i+\tilde{B}B\gamma_i=0. \tag{26}$$

From (25) and (26) and using the fact that $\left[\tilde{B}^T,\bar{B}^T\right]^T$ is nonsingular, it implies

$$Ah_i-\dot{h}_i+B\gamma_i=0\ \forall i\in F \tag{27}$$

which can be rewritten in a compact form

$$[I_M\otimes A]\,h_F-(I_M\otimes I_n)\dot{h}_F+(I_M\otimes B)\,\gamma=0. \tag{28}$$

Premultiplying both sides of (28) by $(C+\rho)\Delta\Xi L_1\otimes P$, we obtain

$$\begin{aligned}&\left[(C+\rho)\Delta\Xi L_1\otimes PA\right]h_F-\left[(C+\rho)\Delta\Xi L_1\otimes P\right]\dot{h}_F\\ &\qquad+\left[(C+\rho)\Delta\Xi L_1\otimes PB\right]\gamma=0.\end{aligned} \tag{29}$$

Substituting (23) and (24) into (22), we get

$$\begin{aligned}\dot{V}_1 \le\ & \xi_F^T[(C+\rho)\Delta\Xi \otimes [PA + A^T P + \Gamma] \\ & - (\lambda_1^{\min}(C+\rho)^2 + \beta\Delta\Xi) \otimes \Gamma]\xi_F \\ & + 2\xi_F^T[(C+\rho)\Delta\Xi L_2 \otimes PB]u_E \\ & - 2\mu\xi_F^T[(C+\rho)\Delta\Xi L_1 \otimes PB]F(\xi).\end{aligned} \tag{30}$$

From (16), it is straightforward to show that

$$\xi_i^T PBf(\xi_i) = \|B^T P\xi_i\| \ \forall i \in F \tag{31}$$

and

$$\begin{aligned}\xi_i^T PBf(\xi_j) \le\ & \|B^T P\xi_i\| \, \|f(\xi_j)\| \ \forall i \ne j \\ \le\ & \|B^T P\xi_i\|\end{aligned} \tag{32}$$

by applying the Cauchy-Schwarz inequality [32]. Subsequently, we have the following relation:

$$\begin{aligned}& -2\mu\xi_F[(C+\rho)\Delta\Xi L_1 \otimes PB]F(\xi) \\ & = -2\mu\sum_{i=1}^{M}(c_i+\rho_i)\varphi_i\xi_i^T PB\sum_{j=1}^{M} w_{ij}[f(\xi_i)-f(\xi_j)] \\ & \quad - 2\mu\sum_{i=1}^{M}(c_i+\rho_i)\varphi_i\sum_{k=M+1}^{N} w_{ik}\xi_i^T PBf(\xi_i) \\ & \le -2\mu\sum_{i=1}^{M}(c_i+\rho_i)\varphi_i\sum_{k=M+1}^{N} w_{ik}\|B^T P\xi_i\|.\end{aligned} \tag{33}$$

Since Assumption 1 holds, it follows that:

$$\begin{aligned}& 2\xi_F[(C+\rho)\Delta\Xi L_2 \otimes PB]u_E \\ & = 2\sum_{i=1}^{M}(c_i+\rho_i)\varphi_i\sum_{k=M+1}^{N} w_{ik}\xi_i^T PBu_k \\ & \le 2\sum_{i=1}^{M}(c_i+\rho_i)\varphi_i\sum_{k=M+1}^{N} w_{ik}\|B^T P\xi_i\|\|u_k\| \\ & \le 2\sigma\sum_{i=1}^{M}(c_i+\rho_i)\varphi_i\sum_{k=M+1}^{N} w_{ik}\|B^T P\xi_i\|.\end{aligned} \tag{34}$$

From Lemma 2, we have

$$\begin{aligned}& -\xi_F^T\left[[\lambda_1^{\min}(C+\rho)^2 + \beta\Delta\Xi] \otimes \Gamma\right]\xi_F \\ & \quad \le -2{\xi_F}^T[\sqrt{\lambda_1^{\min}\beta\Delta\Xi}(C+\rho) \otimes \Gamma]\xi_F.\end{aligned} \tag{35}$$

Selecting $\beta \ge \frac{\max_{i\in F}\varphi_i}{\lambda_1^{\min}}$ and $\mu > \sigma$, the inequality given in (30) implies

$$\dot{V}_1 \le {\xi_F}^T\left[(C+\rho)\Delta\Xi \otimes [PA + A^T P - \Gamma]\right]\xi_F \tag{36}$$

invoking (33)–(35). Now, (36) can be simplified to

$$\dot{V}_1 \le {\zeta_F}^T\left[I_M \otimes (PA + A^T P - PBR^{-1}B^T P)\right]\zeta_F \tag{37}$$

by applying the change of variable $\zeta_F = (\sqrt{(C+\rho)\Delta\Xi} \otimes I)\xi_F$. This implies $\dot{V}_1 \le 0$, since from (15), $PA + A^T P - PBR^{-1}B^T P = -Q < 0$ for given $Q > 0$ and $R > 0$. Also, from (37), $\dot{V}_1 = 0$ only when $\zeta_F = 0$. This implies asymptotic stability of (20) in closed-loop, invoking LaSalle's invariance principle [32]. Therefore, $\lim_{t\to\infty}\zeta_F(t) = 0$ and hence

$$\lim_{t\to\infty}\xi_F(t) = 0 \tag{38}$$

since ζ_F and ξ_F are related via nonsingular transformation.

From (19) and (38), one gets

$$\lim_{t\to\infty}\left[x_F(t) - h_F(t) - (-L_1^{-1}L_2 \otimes I_n)x_E(t)\right] = 0. \tag{39}$$

Applying Lemma 3, (39) can be rewritten as

$$\lim_{t\to\infty}\left[x_F(t) - h_F(t) - \left(\begin{bmatrix} e_1 & 0 & \cdots & 0 \\ 0 & e_2 & \cdots & 0 \\ \vdots & \vdots & \ddots & \vdots \\ 0 & 0 & \cdots & e_p \end{bmatrix} \otimes I_n\right)x_E(t)\right] = 0. \tag{40}$$

Rearranging (40), we have

$$\lim_{t\to\infty}\left(\begin{bmatrix} \bar{x}_1(t) - \bar{h}_1(t) - (e_1 \otimes I_n)\hat{x}_1 \\ \vdots \\ \bar{x}_p(t) - \bar{h}_p(t) - (e_p \otimes I_n)\hat{x}_p \end{bmatrix}\right) = 0, \tag{41}$$

that is, for any $\bar{i} \in \{1, 2, \ldots, p\}$

$$\lim_{t\to\infty}\left[\bar{x}_{\bar{i}}(t) - \bar{h}_{\bar{i}}(t) - \mathbf{1}_{n_{\bar{i}}}\sum_{k=\hat{\varsigma}_{\bar{i}}+1}^{\hat{\varsigma}_{\bar{i}}+\hat{n}_{\bar{i}}}\left(\frac{b_k}{\sum_{j=\hat{\varsigma}_{\bar{i}}+1}^{\hat{\varsigma}_{\bar{i}}+\hat{n}_{\bar{i}}} b_j}x_k(t)\right)\right] = 0. \tag{42}$$

Hence, it can be concluded that the predefined time-varying subformation $\bar{h}_{\bar{i}}$ is achieved by all subgroups and the followers in each subgroup track a convex combination of the states of the respective leaders. This completes the proof. ■

Remark 2: As the formation feasibility condition given in (14) imposes some constraints on the dynamics of the agents and the communication topology, not all types of time-varying formations may be achieved by the followers. In order to design the TGFT protocol, the formation feasibility condition needs to be satisfied *a priori*, which signifies that a desired formation must be compatible with the dynamics of the agents.

Remark 3: In contrast to the results reported in [27], where only "group formation stabilization" problems are addressed, the nonlinear, adaptive control protocol designed in this paper can be used to deal with "group formation tracking" problems as well. Also, direct computation of the smallest positive eigenvalue of the Laplacian matrix is avoided in the proposed scheme, which uses only relative state information with respect to the neighbors. In virtue of this, the proposed control scheme becomes scalable and reconfigurable for large-scale networked systems.

Algorithm 1: Procedure to Design the Control Law for TGFT Problem Involving Multiple Leaders.

1: **for** each agent $i \in \{1, \ldots, M\}$ **do**
2: suppose the MAS (2) satisfies Assumptions 1-4;
3: select the desired formation reference $h_i(t) \in \mathbb{R}^n\ \forall t \geq 0$;
4: **if** formation feasibility condition (14) is satisfied **then**
5: choose a positive constant $\mu > \sigma$ for a given $\sigma \geq 0$;
6: find $P > 0$ by solving the ARE (15) for given $Q > 0$ and $R > 0$;
7: compute the controller gain matrices K and Γ, and the smooth function ρ_i using $P > 0$;
8: choose the matrices $\tilde{B}$ and $\bar{B}$ such that $\tilde{B}B = I_m$ and $\bar{B}B = 0$. Then find γ_i using $\dot{h}_i$, h_i and the matrices $\tilde{B}$ and $\bar{B}$;
9: design the nonlinear function $f(\cdot)$ based on (16);
10: construct the adaptive and nonlinear control protocol u_i given in (3);
11: **else**
12: back to Step 3;
13: **end if**
14: **end for**

Remark 4: When $\hat{n}_{\bar{i}} = 1\ \forall \bar{i} \in \{1, 2, \ldots, p\}$, Theorem 1 specializes in cluster control problems as discussed in [24]–[26]. If $p = 1$, it is straightforward to assert that the TGFT problem reduces to the formation tracking problem with multiple leaders as done in [33]. In the case where $p = 1$ and $M = N - 1$, Theorem 1 can be applied to deal with the standard formation tracking problem [20]. It can further be noted that the TGFT problem solved in this paper reduces to the consensus problem, as discussed in [23] and [30], when $h_i = 0\ \forall i \in \{1, \ldots, M\}$, $p = 1$, and $M = N - 1$. Therefore, the consensus problem, formation problem, and cluster problem can all be viewed as special cases of the TGFT problem addressed in this paper.

Remark 5: In [23], a fully distributed observer–based control law is proposed to solve the cooperative output regulation problem for a class of linear MAS with heterogeneous subsystems. In contrast to [23], this paper deals with TGFT problems which lead to "sub-formation" and "tracking". Moreover, in this paper, a distributed, adaptive, and nonlinear state feedback control protocol has been designed to handle the situations where each subgroup can be assigned multiple leaders, and the leaders may be influenced by unknown exogenous inputs.

Following Theorem 1, a systematic procedure to construct the control law u_i is given in Algorithm 1.

IV. Application: Multitarget Surveillance of Nonholonomic Mobile Robots

In this section, the proposed TGFT control protocol has been utilized to solve a multitarget surveillance problem for a group of nonholonomic mobile robots.

A. Robot Dynamics

Let us consider a scenario where 12 nonholonomic mobile robots are engaged in a multitarget surveillance operation in a 2-D plane. Each robot is assumed to possess the same dynamics and structure, and they are described by the following first-order differential equations in terms of the global coordinates as:

$$\dot{x}_{xi} = v_i \cos\theta_i$$
$$\dot{x}_{yi} = v_i \sin\theta_i$$
$$\dot{\theta}_i = \omega_i \quad \forall i \in \{1, \ldots, 12\}$$

where x_{xi} and x_{yi} together represent the position of the ith robot in the $X - Y$ plane (i.e., in Cartesian coordinates); v_i and ω_i denote, respectively, the linear and angular velocities; and θ_i represents the heading angle measured in an anticlockwise sense from the positive X axis.

To avoid saturation of the electric motors, the linear velocity of each mobile robot is constrained to

$$v_i \leq v_{\max}$$

where $v_{\max} = 10$ m/s is the velocity limit.

For each mobile robot, we introduce a new control input q_i such that

$$\dot{v}_i = q_i.$$

Define $v_{xi} = v_i \cos\theta_i$ and $v_{yi} = v_i \sin\theta_i$ as the components of the linear velocity along the X and Y directions, respectively. Then, we have $\dot{x}_{xi} = v_{xi}$ and $\dot{x}_{yi} = v_{yi}$. The dynamics can be expressed in terms of q_i and ω_i as

$$\begin{bmatrix} \dot{v}_{xi} \\ \dot{v}_{yi} \end{bmatrix} = \begin{bmatrix} \cos\theta_i & -v_i \sin\theta_i \\ \sin\theta_i & v_i \cos\theta_i \end{bmatrix} \begin{bmatrix} q_i \\ \omega_i \end{bmatrix}.$$

Assuming $v_i \neq 0$, the control input is designed as

$$\begin{bmatrix} q_i \\ \omega_i \end{bmatrix} = \begin{bmatrix} \cos\theta_i & \sin\theta_i \\ -\frac{\sin\theta_i}{v_i} & -\frac{\cos\theta_i}{v_i} \end{bmatrix} \begin{bmatrix} u_{xi} \\ u_{yi} \end{bmatrix}.$$

Now, applying feedback linearization, we obtain the linearized state-space model for each mobile robot (including the followers and leaders) which conforms to (2) with $x_i = [x_{xi}^T, v_{xi}^T, x_{yi}^T, v_{yi}^T]^T$ and $u_i = [u_{xi}^T, u_{yi}^T]^T$ and the matrices A and B are given by

$$A = \begin{bmatrix} 0 & 1 & 0 & 0 \\ 0 & 0 & 0 & 0 \\ 0 & 0 & 0 & 1 \\ 0 & 0 & 0 & 0 \end{bmatrix}, \quad B = \begin{bmatrix} 0 & 0 \\ 1 & 0 \\ 0 & 0 \\ 0 & 1 \end{bmatrix}.$$

B. Group Formation and Tracking

In this case study, it is assumed that there are four targets (labelled as 13, 14, 15, 16) moving in the same direction during the first 60 s. After that, due to bounded external disturbances, the targets start moving away from each other. In the first stage (0-60 s), the follower robots are expected to build a circular formation surrounding all four targets (considered as leaders). After 60 s, the followers are divided into three subgroups to form

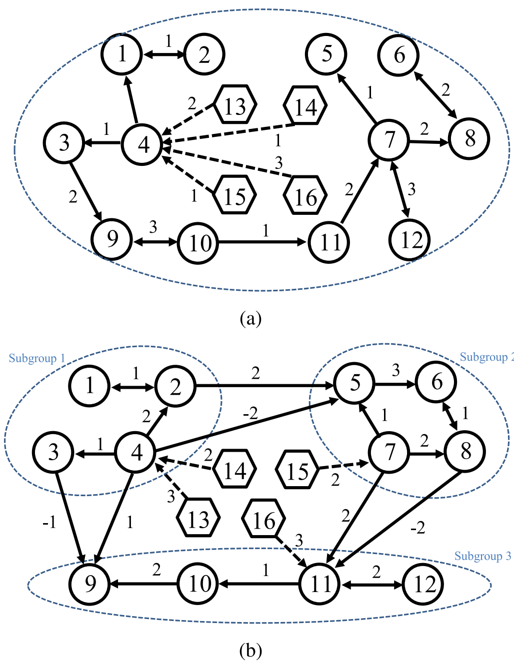

Fig. 1. Interaction topology (a) before 60s and (b) after 60s.

individual sub-formations around each target for better monitoring as the targets start moving away in arbitrary directions due to the effect of external disturbance.

Case I (Complete formation, 0–60 s): The graph shown in Fig. 1(a) illustrates the interconnection of the robots engaged in the surveillance operation. The time-varying circular formation for the follower robots is specified by

$$h_i(t) = \begin{bmatrix} r\sin\left(wt + \frac{2(i-1)\pi}{12}\right) \\ wr\cos\left(wt + \frac{2(i-1)\pi}{12}\right) \\ r\cos\left(wt + \frac{2(i-1)\pi}{12}\right) \\ -wr\sin\left(wt + \frac{2(i-1)\pi}{12}\right) \end{bmatrix} \quad \forall i \in \{1, 2, \ldots, 12\},$$

where $r = 20$ m and $w = 0.1$ rad/s.

Let us choose

$$\tilde{B} = \begin{bmatrix} 0 & 1 & 0 & 0 \\ 0 & 0 & 0 & 1 \end{bmatrix}$$

and

$$\bar{B} = \begin{bmatrix} 1 & 0 & 0 & 0 \\ 0 & 0 & 1 & 0 \end{bmatrix},$$

such that $\tilde{B}B = I_2$ and $\bar{B}B = 0$. Note that this choice of $\bar{B}$ and $h_i(t)$ satisfies the formation feasibility condition (14) given in Theorem 1.

We choose

$$Q = \begin{bmatrix} 0.05 & 0 & 0 & 0 \\ 0 & 0.01 & 0 & 0 \\ 0 & 0 & 0.2 & 0 \\ 0 & 0 & 0 & 0.01 \end{bmatrix}$$

and $R = \left[\begin{smallmatrix} 1 & 0 \\ 0 & 1 \end{smallmatrix}\right]$, and on solving the ARE (15), we get

$$P = \begin{bmatrix} 0.1512 & 0.2236 & 0 & 0 \\ 0.2236 & 0.6762 & 0 & 0 \\ 0 & 0 & 0.4253 & 0.4472 \\ 0 & 0 & 0.4472 & 0.9510 \end{bmatrix} > 0.$$

The controller gain matrices are then calculated as

$$K = \begin{bmatrix} -0.2236 & -0.6762 & 0 & 0 \\ 0 & 0 & -0.4472 & -0.9510 \end{bmatrix}$$

and

$$\Gamma = \begin{bmatrix} 0.0500 & 0.1512 & 0 & 0 \\ 0.1512 & 0.4572 & 0 & 0 \\ 0 & 0 & 0.2000 & 0.4253 \\ 0 & 0 & 0.4253 & 0.9044 \end{bmatrix}.$$

$\mu = 1$ is selected for a given $\sigma = 0.5$ and the nonlinear functions $f(\xi_i)$ are also constructed according to (9) to form the TGFT control protocol (3). The function ρ_i is computed as

$$\rho_i = \xi_i^T \begin{bmatrix} 0.1512 & 0.2236 & 0 & 0 \\ 0.2236 & 0.6762 & 0 & 0 \\ 0 & 0 & 0.4253 & 0.4472 \\ 0 & 0 & 0.4472 & 0.9510 \end{bmatrix} \xi_i,$$

and γ_i is obtained as

$$\gamma_i = \begin{bmatrix} -0.2\sin\left(0.1t + \frac{2(i-1)\pi}{12}\right) \\ -0.2\cos\left(0.1t + \frac{2(i-1)\pi}{12}\right) \end{bmatrix} \quad \forall i \in \{1, 2, \ldots, 12\}.$$

Fig. 2 shows that the follower robots $\forall i \in \{1, 2, \ldots, 12\}$ gradually attain the circular formation specified by $h_i(t)$, starting from arbitrary initial positions. Moreover, the formation continues to revolve around the targets.

Case II (Subformations, 60-100s): These 12 mobile robots are divided into three subgroups, namely, $\mathcal{V}_1 = \{1, 2, 3, 4\}$, $\mathcal{V}_2 = \{5, 6, 7, 8\}$, and $\mathcal{V}_3 = \{9, 10, 11, 12\}$-depending on the relative positions of the targets. $\mathcal{V}_1$ has been assigned two targets (13 and 14), while $\mathcal{V}_2$ and $\mathcal{V}_3$ each have one target. Fig. 1(b) shows the modified interaction topology corresponding to Case II. The desired time-varying subformations for all three subgroups are specified by

$$h_i(t) = \begin{cases} \begin{bmatrix} 20\sin(0.1t + 2(i-1)\pi/4) \\ 2\cos(0.1t + 2(i-1)\pi/4) \\ 20\cos(0.1t + 2(i-1)\pi/4) \\ -2\sin(0.1t + 2(i-1)\pi/4) \end{bmatrix} & i \in \mathcal{V}_1 \\ \begin{bmatrix} 15\sin(0.2t + 2(i-1)\pi/4) \\ 3\cos(0.2t + 2(i-1)\pi/4) \\ 15\cos(0.2t + 2(i-1)\pi/4) \\ -3\sin(0.2t + 2(i-1)\pi/4) \end{bmatrix} & i \in \mathcal{V}_2 \\ \begin{bmatrix} 10\sin(0.3t + 2(i-1)\pi/4) \\ 3\cos(0.3t + 2(i-1)\pi/4) \\ 10\cos(0.3t + 2(i-1)\pi/4) \\ -3\sin(0.3t + 2(i-1)\pi/4) \end{bmatrix} & i \in \mathcal{V}_3. \end{cases}$$

For the same $\tilde{B}$, $\bar{B}$ and other controller parameters as taken in Case I, it can be readily verified that the subformations specified by $h_i(t)$ above, for all $i \in \mathcal{V}_1$, $\mathcal{V}_2$, and $\mathcal{V}_3$, satisfy the

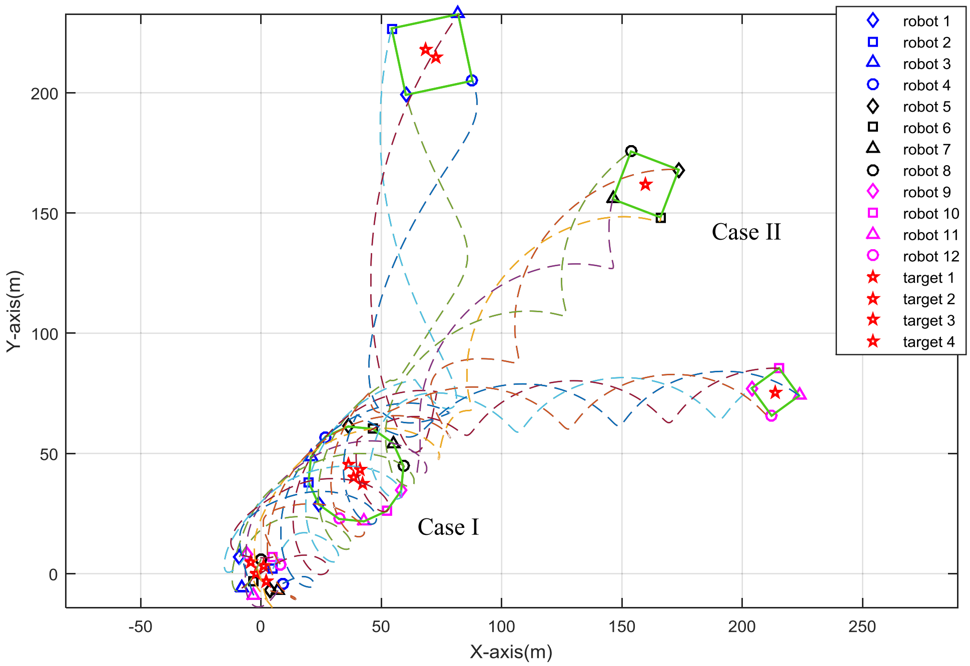

Fig. 2. Formation and subformation diagrams for the multirobot system in the $X - Y$ plane.

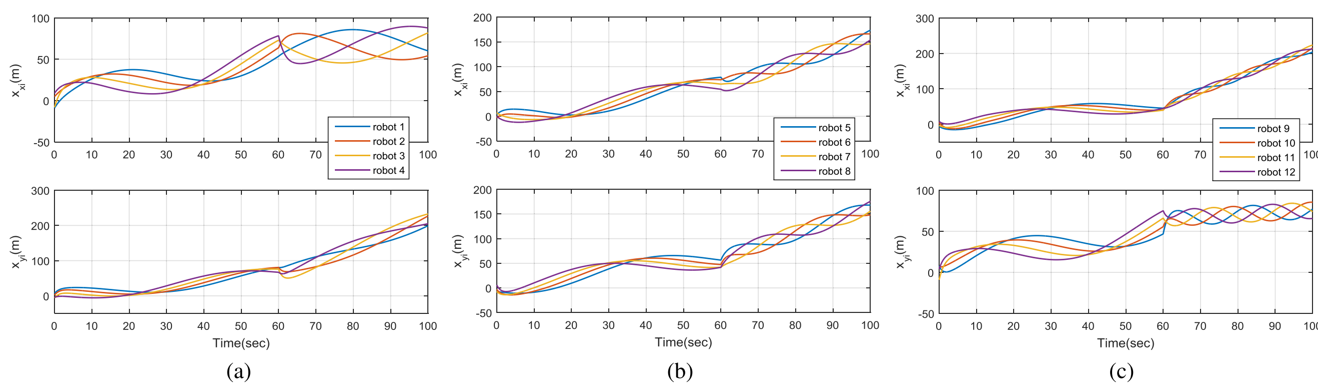

Fig. 3. Time evolvement of the positions of the follower robots belonging to (a) Subgroup 1, (b) Subgroup 2, and (c) Subgroup 3.

group formation feasibility constraint (14) and, hence, each subgroup will achieve the individual subformations according to Theorem 1. The functions γ_i for all $i \in \{1, \ldots, 12\}$ are mentioned below as

$$\gamma_i = \begin{cases} \begin{bmatrix} -0.2\sin\left(0.1t + \frac{2(i-1)\pi}{4}\right) \\ -0.2\cos\left(0.1t + \frac{2(i-1)\pi}{4}\right) \end{bmatrix} & i \in \mathcal{V}_1 \\ \begin{bmatrix} -0.6\sin\left(0.2t + \frac{2(i-1)\pi}{4}\right) \\ -0.6\cos\left(0.2t + \frac{2(i-1)\pi}{4}\right) \end{bmatrix} & i \in \mathcal{V}_2 \\ \begin{bmatrix} -0.9\sin\left(0.3t + \frac{2(i-1)\pi}{4}\right) \\ -0.9\cos\left(0.3t + \frac{2(i-1)\pi}{4}\right) \end{bmatrix} & i \in \mathcal{V}_3. \end{cases}$$

The time evolution of the spatial positions of the robots (both the followers and the targets) are plotted in Fig. 2 which reveals that for $t \leq 60$ s, the follower robots $(1, 2, \ldots, 12)$ together give rise to a dodecagon-shaped formation and keep rotating around the four targets. Fig. 4 depicts the time variations of the coupling weights $c_i(t)$ $\forall i \in \{1, 2, \ldots, 12\}$ which shows that the coupling weights remain bounded $\forall t \geq 0$ and they converge to finite positive values within finite time. Fig. 5 illustrates that the 2-norm of the group formation tracking error $\xi_i(t)$ for each follower decays sharply to zero within finite time which

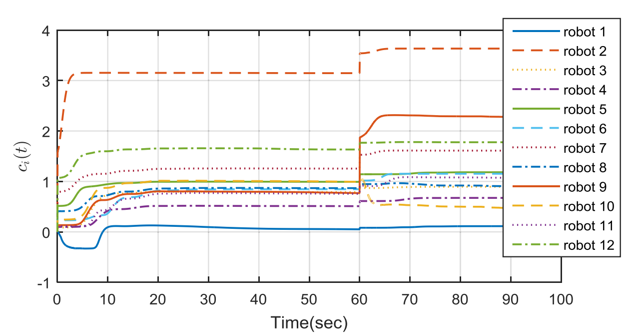

Fig. 4. Variation of the coupling gains c_i with respect to time.

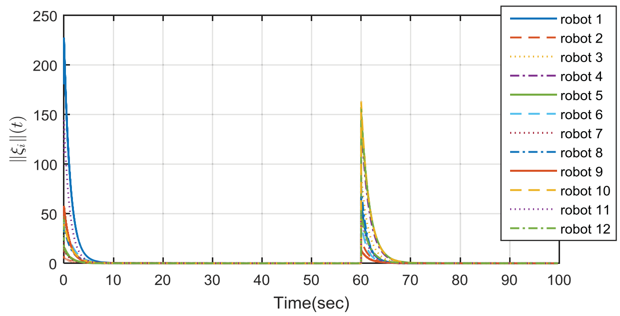

Fig. 5. Time-variation of 2-norms of the group formation tracking errors ξ_i.

confirms that the followers are able to track a convex combination of the positions of the targets. After $t > 60$ s, we observe that three subgroups are formed and they eventually attain the predefined time-varying circular subformations surrounding the respective targets. Fig 4 shows that for $t > 60$ s, the coupling weights adapt to a new set of finite values to counteract the changeover from complete formation to subformation. Thus, TGFT involving multiple targets is achieved by the TGFT control protocol introduced in this paper. Henceforth, it can be concluded that the multitarget surveillance operation is accomplished by the designed control law.

V. Conclusion

A distributed, adaptive, and nonlinear control protocol has been introduced in this paper to achieve TGFT for linear MAS having a directed communication topology. The control objectives also include subformation and tracking, that is, the followers are divided into several subgroups depending on the positions of the leaders and each subgroup reaches individual subformations while tracking the positions of the respective leaders attached to that subgroup. In contrast to existing literature, this paper addresses the group formation tracking problem where each subgroup can have multiple leaders and the leaders may have separate control inputs. The proposed scheme finds a lot of applications in swarm robotics especially in multitarget surveillance operations where the targets (considered as leaders) may be placed far apart and sometimes the targets may keep on changing their positions due to an external disturbance. In order to tackle such constraints, in this paper, each target considers a bounded exogenous input (reference or disturbance) in its dynamic model instead of being characterized as an autonomous system. The proposed control technique is fully distributed since it requires only the relative state information and does not need to calculate the eigenvalues of the graph Laplacian. The advantage of using an appropriate blending of adaptive and nonlinear control techniques is to render the proposed control scheme robust to network topology changes because in the future, this work may be extended to deal with parameter variations and model uncertainties of the agents. Moreover, the TGFT problem should also be extended tor heterogeneous MAS.

References

[1] H. A. Poonawala, A. C. Satici, H. Eckert, and M. W. Spong, "Collision-free formation control with decentralized connectivity preservation for nonholonomic-wheeled mobile robots," *IEEE Trans. Control Netw. Syst.*, vol. 2, no. 2, pp. 122–130, Jun. 2015.

[2] A. Nagendran, W. Crowther, M. Turner, A. Lanzon, and R. Richardson, "Design, control, and performance of the 'weed' 6 wheel robot in the UK MOD grand challenge," *Adv. Robot.*, vol. 28, no. 4, pp. 203–218, 2014.

[3] B. Crowther, A. Lanzon, M. Maya-Gonzalez, and D. Langkamp, "Kinematic analysis and control design for a nonplanar multirotor vehicle," *AIAA J. Guidance, Control, Dyn.*, vol. 34, no. 4, pp. 1157–1171, 2011.

[4] G. Foderaro, P. Zhu, H. Wei, T. A. Wettergren, and S. Ferrari, "Distributed optimal control of sensor networks for dynamic target tracking," *IEEE Trans. Control Netw. Syst.*, vol. 5, no. 1, pp. 142–153, Mar. 2018.

[5] R. Deng, S. He, and J. Chen, "An online algorithm for data collection by multiple sinks in wireless-sensor networks," *IEEE Trans. Control Netw. Syst.*, vol. 5, no. 1, pp. 93–104, Mar. 2018.

[6] J. Hu and A. Lanzon, "Distributed finite-time consensus control for heterogeneous battery energy storage systems in droop-controlled microgrids," *IEEE Trans. Smart Grid*, 2018, doi:10.1109/TSG.2018.2868112.

[7] J. Wang, A. Lanzon, and I. R. Petersen, "Robust output feedback consensus for networked negative-imaginary systems," *IEEE Trans. Autom. Control*, vol. 60, no. 9, pp. 2547–2552, Sep. 2015.

[8] J. Sun, Z. Geng, Y. Lv, Z. Li, and Z. Ding, "Distributed adaptive consensus disturbance rejection for multi-agent systems on directed graphs," *IEEE Trans. Control Netw. Syst.*, vol. 5, no. 1, pp. 629–639, Mar. 2018.

[9] J. Wang, A. Lanzon, and I. R. Petersen, "Robust cooperative control of multiple heterogeneous negative-imaginary systems," *Automatica*, vol. 61, pp. 64–72, 2015.

[10] Z. Li, Z. Duan, W. Ren, and G. Feng, "Containment control of linear multi-agent systems with multiple leaders of bounded inputs using distributed continuous controllers," *Int. J. Robust Nonlinear Control*, vol. 25, no. 13, pp. 2101–2121, 2015.

[11] S. Zuo, Y. Song, F. L. Lewis, and A. Davoudi, "Time-varying output formation-containment of general linear homogeneous and heterogeneous multi-agent systems," *IEEE Trans. Control Netw. Syst.*, 2018, doi: 10.1109/TCNS.2018.2847039.

[12] S. Zhao and D. Zelazo, "Translational and scaling formation maneuver control via a bearing-based approach," *IEEE Trans. Control Netw. Syst.*, vol. 4, no. 3, pp. 429–438, Sep. 2017.

[13] M. Turpin, N. Michael, and V. Kumar, "Decentralized formation control with variable shapes for aerial robots," in *Proc. IEEE Int. Conf. Robot. Autom.*, Saint Paul, MN, USA, 2012, pp. 23–30.

[14] M. H. Trinh, S. Zhao, Z. Sun, D. Zelazo, B. D. Anderson, and H.-S. Ahn, "Bearing-based formation control of a group of agents with leader-first follower structure," *IEEE Trans. Autom. Control*, vol. 64, no. 2, Feb. 2019, pp. 598–613, doi: 10.1109/TAC.2018.2836022.

[15] C. Wang, H. Tnunay, Z. Zuo, B. Lennox, and Z. Ding, "Fixed-time formation control of multi-robot systems: Design and experiments," *IEEE Trans. Ind. Electron.*, vol. 66, no. 8, pp. 6292–6301, Aug. 2019, doi: 10.1109/TIE.2018.2870409.

[16] X. Li and L. Xie, "Dynamic formation control over directed networks using graphical laplacian approach," *IEEE Trans. Autom. Control*, vol. 63, no. 11, pp. 3761–3774, Nov. 2018, doi: 10.1109/TAC.2018.2798808.

[17] S. Zhao, "Affine formation maneuver control of multi-agent systems," *IEEE Trans. Autom. Control*, vol. 63, no. 12, pp. 4140–4155, Dec. 2018, doi:10.1109/TAC.2018.2798805.

[18] X. Dong, B. Yu, Z. Shi, and Y. Zhong, "Time-varying formation control for unmanned aerial vehicles: Theories and applications," *IEEE Trans. Control Syst. Technol.*, vol. 23, no. 1, pp. 340–348, Jan. 2015.

[19] X. Dong, Y. Zhou, Z. Ren, and Y. Zhong, "Time-varying formation tracking for second-order multi-agent systems subjected to switching topologies with application to quadrotor formation flying," *IEEE Trans. Ind. Electron.*, vol. 64, no. 6, pp. 5014–5024, Jun. 2017.

[20] J. Hu and A. Lanzon, "An innovative tri-rotor drone and associated distributed aerial drone swarm control," *Robot. Auton. Syst.*, vol. 103, pp. 162–174, 2018.

[21] Z. Li and Z. Duan, *Cooperative Control of Multi-agent Systems: A Consensus Region Approach*. Boca Raton, FL, USA: CRC, 2014.

[22] R. Wang, X. Dong, Q. Li, and Z. Ren, "Distributed adaptive time-varying formation for multi-agent systems with general high-order linear time-invariant dynamics," *J. Franklin Inst.*, vol. 353, no. 10, pp. 2290–2304, 2016.

[23] Z. Li, M. Z. Chen, and Z. Ding, "Distributed adaptive controllers for cooperative output regulation of heterogeneous agents over directed graphs," *Automatica*, vol. 68, pp. 179–183, 2016.
[24] W. Xia and M. Cao, "Clustering in diffusively coupled networks," *Automatica*, vol. 47, no. 11, pp. 2395–2405, 2011.
[25] Y. Feng, S. Xu, and B. Zhang, "Group consensus control for double-integrator dynamic multiagent systems with fixed communication topology," *Int. J. Robust Nonlinear Control*, vol. 24, no. 3, pp. 532–547, 2014.
[26] J. Qin and C. Yu, "Cluster consensus control of generic linear multi-agent systems under directed topology with acyclic partition," *Automatica*, vol. 49, no. 9, pp. 2898–2905, 2013.
[27] X. Dong, Q. Li, Q. Zhao, and Z. Ren, "Time-varying group formation analysis and design for second-order multi-agent systems with directed topologies," *Neurocomputing*, vol. 205, pp. 367–374, 2016.
[28] H. Zhang, F. L. Lewis, and Z. Qu, "Lyapunov, adaptive, and optimal design techniques for cooperative systems on directed communication graphs," *IEEE Trans. Ind. Electron.*, vol. 59, no. 7, pp. 3026–3041, Jul. 2012.
[29] D. S. Bernstein, *Matrix Mathematics: Theory, Facts, and Formulas with Application to Linear Systems Theory*. Princeton, NJ, USA: Princeton Univ. Press, 2005.
[30] Y. Lv, Z. Li, Z. Duan, and G. Feng, "Novel distributed robust adaptive consensus protocols for linear multi-agent systems with directed graphs and external disturbances," *Int. J. Control*, vol. 90, no. 2, pp. 137–147, 2017.
[31] F. Zhang, *The Schur Complement and its Applications*. Berlin, Germany: Springer Science & Business Media, 2006.
[32] H. K. Khalil, *Noninear Systems*. Upper Saddle River, NJ, USA: Prentice-Hall, 1996.
[33] X. Dong and G. Hu, "Time-varying formation tracking for linear multi-agent systems with multiple leaders," *IEEE Trans. Autom. Control*, vol. 62, no. 7, pp. 3658–3664, Jul. 2017.

Junyan Hu received the B.Eng degree in automation from Hefei University of Technology, Hefei, China, in 2015 and the M.Sc degree in advanced control and system engineering from the University of Manchester, Manchester, U.K., in 2016, where he is currently working toward the Ph.D degree in electrical and electronic engineering.

His research interests include cooperative control of multiagent dynamical systems and control application for unmanned aerial vehicles and autonomous mobile robots.

Mr. Hu serves as a Reviewer for a number of international journals, including IEEE TRANSACTIONS ON ROBOTICS, IEEE TRANSACTIONS ON CYBERNETICS, IEEE TRANSACTIONS ON SMART GRID, and IEEE TRANSACTIONS ON POWER SYSTEMS.

Parijat Bhowmick received the B.Tech. degree in electrical engineering from West Bengal University of Technology, Kolkata, India, in 2008, the M.E. degree in control systems engineering from Jadavpur University, Kolkata, India, in 2012, and the Ph.D. degree in control engineering from Indian Institute of Technology Kharagpur, India, in 2018.

Currently, he is a Postdoctoral Research Associate with the School of Electrical and Electronic Engineering, University of Manchester, Manchester, U.K. His research interests include robust control of negative-imaginary systems, passivity-based control, and decentralized integral control.

Alexander Lanzon (SM'07) received the Ph.D. degree in control engineering and the M.Phil. degree in robot control from the University of Cambridge, Cambridge, U.K., in 2000 and 1997, respectively and the B.Eng.(Hons). degree in electrical and electronic engineering from the University of Malta, Msida, Malta, in 1995.

He has held research and academic positions at the Georgia Institute of Technology, Atlanta GA, USA, and the Australian National University, Canberra ACT, Australia, and industrial positions at ST-Microelectronics Ltd., Kirkop, Malta; Yaskawa Denki (Tokyo) Ltd., Saitama-Ken, Japan; and National ICT Australia Ltd., Canberra ACT, Australia. In 2006, he joined the University of Manchester, Manchester, U.K., where he now holds the Chair in control engineering. His research interests include the fundamentals of feedback control theory, negative imaginary systems theory, $\mathcal{H}_\infty$ control theory, robust linear and nonlinear feedback control systems, and applying robust control theory to innovative mechatronic, robotic, and drone applications.

Prof. Lanzon is a Fellow of the Institute of Mathematics and its Applications, the Institute of Measurement and Control, and the Institution of Engineering and Technology. He served as an Associate Editor of the IEEE TRANSACTIONS ON AUTOMATIC CONTROL from 2012 to 2018, and as a Subject Editor of the *International Journal of Robust and Nonlinear Control* from 2012 to 2015.